ALCHEMY Jurnal Penelitian Kimia

Official Website: https://jurnal.uns.ac.id/alchemy

ISSN 1412-4092
EISSN 2443-4183

Optimization and Evaluation of Polymer Inclusion Membrane (PIM) Containing 10% Copoly Eugenol Divinyl Benzene as Carrier Compound for Malachite Green Transport

Agung Abadi Kiswandono*, Kharisma Citra Aprilia, Rinawati Rinawati, Hardoko Insan Qudus, Suharso Suharso

Department of Chemistry, Faculty of Mathematics and Natural Sciences, Lampung University
Jalan Prof. Dr. Sumantri Brojonegoro No. 1, Bandar Lampung, Lampung 35144, Indonesia

Corresponding author: agung.abadi@fmipa.unila.ac.id

DOI: 10.20961/alchemy.22.2.112200.479-491

Received 7 December 2025, Revised 29 January 2026, Accepted 8 February 2026, Published 30 September 2026

Keywords:

carrier;
malachite green;
polymer inclusion membrane.

ABSTRACT. This study investigated the optimization of a Polymer Inclusion Membrane (PIM) for Malachite Green (MG) transport by evaluating the effects of source-phase pH, receiving-phase concentration, membrane thickness, carrier concentration, and transport time. The PIM was prepared using 10% copoly eugenol divinyl benzene (Co-EDVB) as the carrier, polyvinyl chloride (PVC) as the base polymer, and dibutyl ether (DBE) as the plasticizer. Transport experiments employed an aqueous MG solution as the source phase and nitric acid (HNO_3) as the receiving phase. Optimal transport conditions were obtained at a source phase pH of 7, a receiving phase concentration of 1.00 M HNO_3, an optimized membrane thickness containing 0.03 mmol carrier, and a transport time of 12 hours, achieving a maximum MG removal efficiency of 85.67%. Transport efficiency increased with pH, carrier concentration, and transport time until reaching optimal conditions, then declined beyond those values. Fourier transform infrared (FTIR) spectroscopy confirmed interactions between MG and membrane components. Scanning electron microscopy (SEM) analysis revealed surface damage and pore formation after transport, indicating partial leaching of membrane components. Overall, these findings emphasize the importance of membrane stability and the optimization of both physical and chemical parameters to enhance MG transport performance in PIM systems.

INTRODUCTION

Industrial development causes environmental pollution and the degradation of natural resources. Synthetic dyes are widely used because they are practical, inexpensive, stable, and bio-oxidation resistant (Ling and Suah, 2017). However, they harm biodiversity and human health by causing irritation, cancer, and mutations. The textile industry is the main source of non-degradable dye waste (Abu-Hussien *et al*., 2022), which contains hazardous substances such as dyes, nitrates, acetic acid, soap, chromium, and toxic heavy metals (Soo *et al*., 2021). Malachite green (MG) is widely used due to its low cost, ease of use, and attractive color. Although effective against bacteria, MG is banned by the United States Food and Drug Administration (US FDA) and Ministerial Decree No. 52/KEPMEN-KP/2014. MG waste blocks light in water, harms aquatic life, and is carcinogenic, genotoxic, mutagenic, and teratogenic (Mazumder and Rano, 2022). MG toxicity increases with time, temperature, and concentration, while the safe water limit is 0.01 ppm (Mohammed *et al*., 2023).

Various MG treatment methods include adsorption with microalgae biochar (Pathy *et al*., 2022), photocatalytic degradation using fly ash–silver oxide nanoparticles (FA-Ag_2O NAP) (Mazumder and Rano, 2022), ozonolysis with titanium dioxide (TiO_2) (Bahrami *et al*., 2020), and separation using Polymer Inclusion Membrane (PIM) (Ling and Suah, 2017). Conventional methods such as coagulation, flocculation, and activated carbon adsorption often show limited effectiveness for MG removal due to its high solubility, stable aromatic structure, and strong interaction with aqueous media (Bahrami *et al*., 2020). In addition, MG is known to be resistant to biodegradation, photodegradation, and repeated washing, which contributes to its persistence in aquatic

Cite this as: Kiswandono, A. A., Aprilia, K. C., Rinawati, R., Qudus, H. I., and Suharso, S. (2026). Optimization and Evaluation of Polymer Inclusion Membrane (PIM) Containing 10% Copoly Eugenol Divinyl Benzene as Carrier Compound for Malachite Green Transport. *ALCHEMY Jurnal Penelitian Kimia*, 22(2), 479-491. doi: https://dx.doi.org/10.20961/alchemy.22.2.112200.479-491.

Copyright © 2026, Universitas Sebelas Maret, ISSN 1412-4092, e ISSN 2443-4183

environments. Liquid membrane systems such as Bulk Liquid Membrane (BLM), Emulsion Liquid Membrane (ELM), Supported Liquid Membrane (SLM), and Polymer Inclusion Membrane (PIM) have therefore been developed as more effective alternatives for MG separation (Ling and Suah, 2017).

PIM is widely used due to its high selectivity, operational simplicity, energy efficiency, and flexibility (Sadiq *et al*., 2023). PIM employs polyvinyl chloride (PVC) as the base polymer to prevent solvent leakage and dibutyl ether (DBE) as a plasticizer to enhance membrane stability (Kiswandono *et al*., 2024b). This system integrates liquid–liquid extraction into a single membrane phase by immobilizing organic solvents within polymer pores (Kiswandono *et al*., 2022). PIM offers advantages such as low carrier consumption, high stability, high flux, and simple operation (Arabi *et al*., 2021). Benosmane *et al*. (2018) reported phenol recovery of up to 95% depending on pH, while Soo *et al*. (2021) demonstrated successful PIM applications in various separation processes, including MG extraction.

Carrier compounds play a key role in separation (Mohammed *et al*., 2023). Poly(eugenol) from eugenol polymerization (Kiswandono *et al*., 2022) contains allyl, hydroxyl, and methoxy groups (Kowalewska and Majewska-Smolarek, 2023). Other carriers such as dioctyl phthalate (DOP) (Soo *et al*., 2021), di-(2-ethylhexyl) phosphoric acid (D2EHPA) (Raval *et al*., 2022), poly(eugenol) (Kiswandono *et al*., 2024b), and 2-aminomethylpyridine (2-AMP) (Qiu *et al*., 2021) are also effective. Polymerization increases molecular weight and active sites such as –OH groups and benzene rings for selective transport (Kiswandono *et al*., 2024a). Copoly eugenol divinylbenzene (Co-EDVB), a diene-based compound, increases active sites and can be synthesized at room temperature (Kiswandono *et al*., 2022). Polymerization with dienes and epoxides forms crosslinked structures (Kowalewska and Majewska-Smolarek, 2023), improving molecular weight and transport efficiency (Carner *et al*., 2020). Previous studies reported 97% MG removal using PIM and bis(2-ethylhexyl) phosphate (B2EHP) (Soo *et al*., 2021), 90% using SLM (Ashraf *et al*., 2019), and 94.99% using ELM and D2EHPA (Raval *et al*., 2022).

Although numerous studies have demonstrated the effectiveness of Polymer Inclusion Membranes (PIMs) for Malachite Green (MG) removal using various carrier compounds, most previous research has primarily focused on achieving high removal efficiency or examining the influence of carrier molecular structure and molecular weight sites. While increasing carrier molecular weight has been reported to enhance membrane stability and transport performance, systematic optimization of operational and membrane parameters remains limited, particularly for newly developed carrier materials (Abu-Hussien *et al*., 2022). To date, there is a lack of comprehensive studies examining the combined effects of source-phase pH, receiving-phase concentration, membrane thickness, carrier concentration, and transport time on MG transport using PIM systems (Soo *et al*., 2021). Moreover, the application of copoly eugenol divinyl benzene (Co-EDVB) as a carrier in PIM, especially at a defined composition of 10%, has rarely been investigated, and its optimal operating conditions have not yet been clearly established (Mazumder and Rano, 2022; Mohammed *et al*., 2023). Therefore, this study aims to fill this research gap by systematically optimizing key transport and membrane parameters for MG separation using a PIM containing 10% Co-EDVB as the carrier. In addition, this study evaluates membrane stability to better understand the relationship between carrier characteristics, operating conditions, and PIM performance. The results are expected to provide practical guidance for the design and optimization of stable and efficient PIM systems for dye removal.

RESEARCH METHODS

The equipment used in this study includes scanning electron microscope (SEM, ZEISS EVO MA 10), Fourier transform infrared spectroscopy (FTIR, Agilent Carry 630), and UV-Vis Spectrophotometer (Lab Junction LJ-2371), analytical digital balance (Mettler Toledo AB54-S), chamber with a diameter of 3.5 cm, pH meter (pH 60 VioLab pH-Mv-Orp-T), 5 cm membrane mold, thickness gauge (Mitutoyo 7301). The materials used in this study include malachite green (MG) (CAS No. 14426-28-9), Synthesis result of Co-EDVB 10%, polyvinyl chloride (PVC) (Ashahimas Chemical), dibenzyl ether (DBE) (Sigma-Aldrich), tetrahydrofuran (THF) (Sigma-Aldrich), nitric acid (HNO_3) (Sigma-Aldrich), lead carbonate ($PbCO_3$) (Sigma-Aldrich), and copper(II) sulfate pentahydrate ($CuSO_4 \cdot 5H_2O$) (Sigma-Aldrich).

PIM Membrane Preparation

The PIM membranes were fabricated with total masses of 0.2700 g, 0.5400 g, and 1.0800 g (Table 1). The membranes were composed of Co-EDVB 10% as the carrier compound, PVC as the base polymer, and DBE as

Copyright © 2026, Universitas Sebelas Maret, ISSN 1412-4092, e ISSN 2443-4183

the plasticizer. Each membrane was dissolved in 10 mL of tetrahydrofuran (THF) to homogenize the mixture in the mold. The membranes were then left undisturbed for three days to allow the solvent to evaporate naturally.

Table 1. Composition ratio of membrane components (10:32:58) (Kiswandono *et al*., 2024a).

Type of Membrane	Co-EDVB (g)	PVC (g)	DBE (g)	Total Mass (g)
T_{27}	0.0270	0.0864	0.1556	0.2700
T_{54}	0.0540	0.1728	0.3132	0.5400
T_{108}	0.1080	0.3456	0.6264	1.0800

After the PIM membrane was cast, it was weighed before use in the MG transport process in the transport chamber. The source phase contained 25 ppm MG solution, while the receiving phase contained HNO_3 as the binding agent. Membrane characterization before and after transport was conducted using FTIR and SEM.

Determination of the Maximum Wavelength of MG

The maximum wavelength of MG was determined by measuring its absorbance over 400–800 nm using a UV-Vis spectrophotometer (Khairati *et al*., 2025). The absorbance of 5 mL samples from the source phase, receiving phase, and standard MG solutions (10, 15, 20, 25, 30, 35, and 40 ppm) was measured at the maximum wavelength.

pH Variation in the Source Phase

The cast PIM membrane was placed in the transport chamber. A total of 50 mL of 1 M HNO_3 was added as the receiving phase, and 50 mL of 25 ppm MG solution was added as the source phase with pH variations of 5, 6, 7, 8, and 9. The system was sealed and stirred for 9 hours using a magnetic stirrer. After the process, 5 mL samples were collected from both phases, and the MG concentrations were measured using a UV-Vis spectrophotometer at the maximum wavelength.

Variation of HNO_3 Concentration

HNO_3 solutions with concentrations of 0.50, 0.75, 1.00, 1.25, and 1.50 M were prepared from 13 M concentrated HNO_3. The PIM membrane was placed in the transport chamber. A total of 50 mL of HNO_3 was added as the receiving phase, and 50 mL of 25 ppm MG solution at the optimum pH was added as the source phase. The system was sealed and stirred for 9 hours. After the process, 5 mL samples were collected from both phases, and the MG concentrations were analyzed using a UV-Vis spectrophotometer at the maximum wavelength.

Variation of Membrane Thickness

PIM membranes with thin (T_{27}), normal (T_{54}), and thick (T_{108}) thicknesses (Kiswandono *et al*., 2020) were tested. A total of 50 mL of HNO_3 at the optimum concentration was added as the receiving phase, and 50 mL of 25 ppm MG solution at the optimum pH was added as the source phase. The system was sealed and stirred for 9 hours. After the process, 5 mL samples were collected from both phases, and the MG concentrations were measured using a UV-Vis spectrophotometer at the maximum wavelength.

Variation of Carrier Amount (mmol)

PIM membranes with optimum thickness and various carrier amounts (Table 2) were tested. A total of 50 mL of HNO_3 at the optimum concentration was added as the receiving phase, and 50 mL of 25 ppm MG solution at the optimum pH was added as the source phase. The system was sealed and stirred for 9 hours. After the process, 5 mL samples were collected from both phases, and the MG concentrations were determined using a UV-Vis spectrophotometer at the maximum wavelength.

Table 2. Total mass of membrane casting solution.

Membrane	Co-EDVB 10 % (mmol)	Mass of Co-EDVB 10% (g)	PVC (g)	DBE (g)
1	0.01	0.0144	0.1728	0.3132
2	0.02	0.0288	0.1728	0.3132
3	0.03	0.0540	0.1728	0.3132
4	0.04	0.0576	0.1728	0.3132
5	0.05	0.0721	0.1728	0.3132

Copyright © 2026, Universitas Sebelas Maret, ISSN 1412-4092, e ISSN 2443-4183

Transport Time Variation

The PIM membrane with optimum thickness and carrier concentration was placed in the center of the transport pipe. Then, 50 mL of HNO_3 at the optimum concentration was added as the receiving phase, and 50 mL of 25 ppm MG solution at the optimum pH was added as the source phase. The transport pipe was sealed and stirred using a magnetic stirrer for 4, 8, 12, 18, and 24 hours. After stirring, 5 mL samples were taken from both phases. MG concentrations were measured using a UV-Vis spectrophotometer at the maximum wavelength.

RESULTS AND DISCUSSION

PIM Membrane Preparation Results

The PIM membrane was prepared with total mass variations: T_{27} (0.2700 g), T_{54} (0.5400 g), and T_{108} (1.0800 g), each producing an orange membrane with a diameter of 4 cm. The membranes were thin, flexible, and sheet-shaped. Membrane thickness was measured using a thickness gauge by placing the sensor on the membrane surface (Khairati *et al*., 2025). The PIM membrane containing Co-EDVB 10% is shown in Figure 1, and the thickness of each fabricated PIM membrane was measured, and the results are presented in Table 3.



(a) (b) (c)

Figure 1. PIM membranes containing Co-EDVB 10% (a) T_{27}, (b) T_{54}, and (c) T_{108}.

Table 3. Total component mass, membrane mass, and PIM membrane thickness before transport.

Type of Membrane	Total Mass (g)	Average Membrane Mass (g)	Average Membrane Thickness (mm)
T_{27} (Thin)	0.2700	0.2426	0.11
T_{54} (Normal)	0.5400	0.4512	0.28
T_{108} (Thick)	1.0800	0.8452	0.43

Maximum Wavelength of MG

The maximum wavelength of MG was determined using a UV-Vis spectrophotometer within the wavelength range of 586 – 642 nm. The measurement results showed that the maximum wavelength of MG was at 614 nm (Figure 2). This wavelength was then used as the operational wavelength for MG concentration analysis in the subsequent tests (Kiswandono *et al*., 2024b).

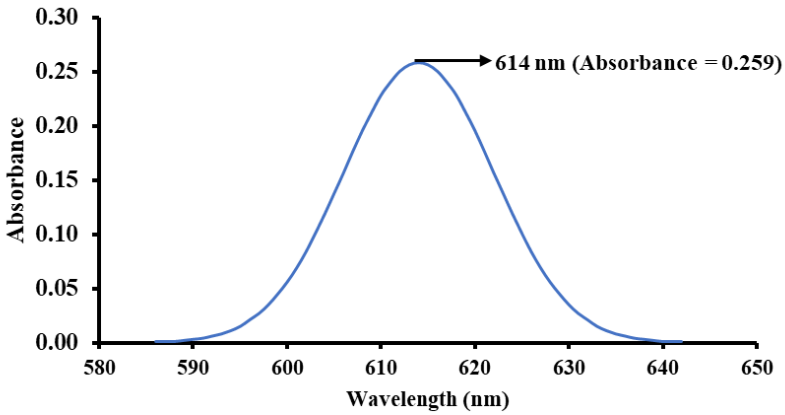


Figure 2. Maximum wavelength of MG.

Several previous studies have reported the maximum wavelength of MG. Bahrami *et al*. (2020) reported a maximum wavelength at 618.07 nm, while Ling and Suah (2017) observed it at 617.0 nm. Minor variations in the

Copyright © 2026, Universitas Sebelas Maret, ISSN 1412-4092, e ISSN 2443-4183

reported maximum wavelength can be attributed to differences in solvent environment, blank composition (distilled water), and instrumental characteristics, such as light source stability and detector sensitivity of the UV–Vis spectrophotometer used.

pH Variation in the Source Phase

The difference in hydrogen ion concentration between the source and receiving phases plays a crucial role in membrane diffusion. Therefore, pH significantly affects MG transport efficiency. In this study, the source phase contained 25 ppm MG solution, the membrane phase used 10% Co-EDVB, and the receiving phase contained 0.1 M HNO_3. The pH of the source phase was varied at 5, 6, 7, 8, and 9 for 9 hours. The MG % removal results were 52.11%, 58.23%, 75.55%, 62.14%, and 52.76%, respectively. The optimum condition occurred at pH 7 with 75.55% removal, where MG tends to form hydrogen bonds that increase solubility and interaction with the carrier in the membrane, enhancing transport efficiency (Khairati *et al*., 2025). This result aligns with Aprilia *et al.* (2025), who found neutral pH to be the most effective for dye separation. Ling and Suah (2017) also reported optimal MG transport at pH 7 – 9. At low pH, transport efficiency decreases due to changes in MG ionic species.

Although chromophore stability of MG may decrease under strongly alkaline conditions, the pH range applied in this study (pH 5 – 9) remains within the operational range commonly reported for spectrophotometric analysis of MG transport. The decrease in removal efficiency observed at higher pH values (pH 8 – 9) is therefore interpreted as a result of changes in MG ionic species and interaction behavior with the membrane, rather than analytical inaccuracy. This interpretation is supported by consistent trends between % removal data and FTIR spectral changes, which confirm specific MG–membrane interactions under different pH conditions. Furthermore, the spectrophotometric method used in this study was applied consistently across all pH variations, ensuring relative comparability of the results. Any potential reduction in chromophore stability would affect all measurements systematically and would not alter the identification of the optimum pH condition. The optimum transport at pH 7 is also corroborated by previous studies reporting neutral pH as the most favorable condition for MG transport (Aprilia *et al*., 2025; Ling and Suah, 2017). The effect of pH in the source phase is presented in Figure 3.

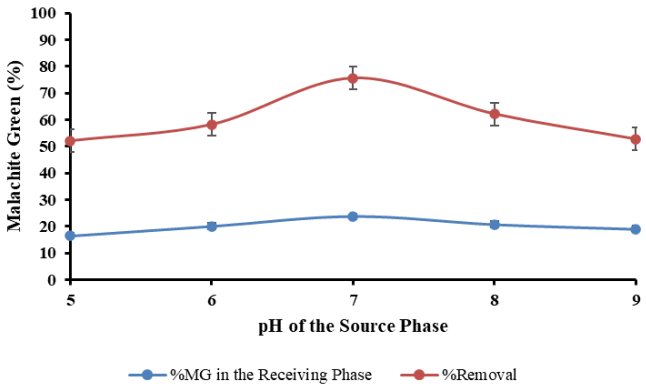


Figure 3. The effect of MG pH in the source phase on the transported MG concentration (%Cs: MG concentration in the source phase; % Removal: MG concentration in the membrane and receiving phases).

Ashraf *et al*. (2019) found that pH changes beyond the optimum condition can cause dissociation of the –OH groups in MG, leading to reduced color intensity due to the loss of chromophore stability. Excessively alkaline conditions may also fade the color because of reactions with the acidic receiving phase. The characterization results of the PIM membrane before and after MG transport at various source phase pH levels are shown in Figure 4.

Figure 4 shows the shift of the O–H or N–H band from 3584.28 cm^{-1} to 3305.77 cm^{-1}, indicating the formation of hydrogen bonding interactions between MG and functional groups in the membrane. Although water molecules may also contribute to hydrogen bonding, the observed band shifts are attributed to MG–membrane interactions, as the spectral changes appear only after MG transport and are accompanied by shifts in aromatic bands associated with MG structure. This suggests that the interactions are not solely due to membrane hydration but involve specific interactions with MG molecules. The disappearance of the aliphatic C–H band at 2929.32 cm^{-1} suggests possible interactions between the alkyl groups of PVC or DBE with MG. The shifts in the aromatic bands from 1650.35 cm^{-1} to 1649.05 cm^{-1} and from 736.82 cm^{-1} to 698.05 cm^{-1} indicate the presence of π–π

Copyright © 2026, Universitas Sebelas Maret, ISSN 1412-4092, e ISSN 2443-4183

stacking interactions (Kiswandono *et al*., 2024b). These FTIR changes confirm that MG transport involves hydrogen bonding and specific interactions with the membrane. Despite the band shifts, the membrane structure remained stable and undamaged during the transport process. This result proves that the membrane effectively recognizes and transports MG, influenced by pH conditions.

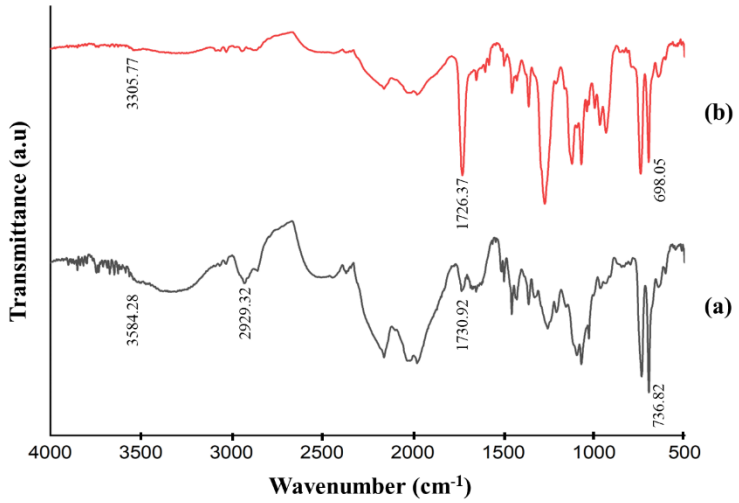


Figure 4. FTIR spectra of the membrane: (a) before transport, (b) after transport with pH variation in the source phase.

Variation of HNO_3 Concentration in the Receiving Phase

The concentration of the receiving phase is a key parameter in optimizing MG transport. This study used HNO_3 solutions with concentrations of 0.50, 0.75, 1.00, 1.25, and 1.50 M at the optimum pH of 7 for 9 hours (Kiswandono *et al*., 2024b). The MG % removal achieved was 75.40%, 75.66%, 76.85%, 74.49%, and 73.32%, respectively. The optimum condition was obtained at 1.00 M HNO_3 with 76.85% MG removal. The HNO_3 concentration is crucial because it generates NO_3^- and H_3O^+ ions. The effect of HNO_3 concentration in the receiving phase on MG transport optimization is shown in Figure 5.

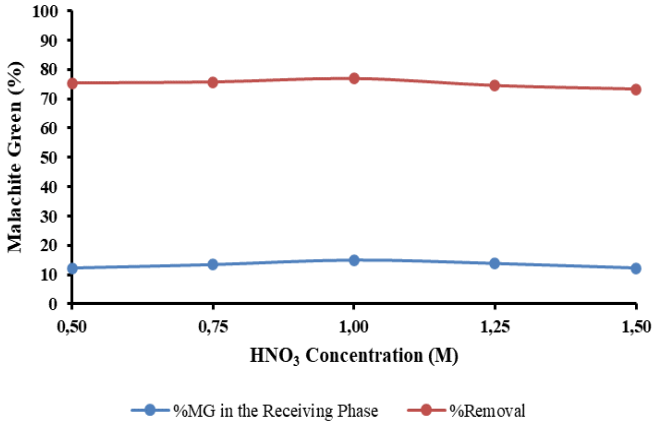


Figure 5. The effect of HNO_3 concentration variation in the receiving phase on the transported MG concentration.

The increase in HNO_3 concentration enhances the stripping ability of the receiving phase by providing protons to release MG from the carrier. However, excessively high HNO_3 concentrations may lead to over-protonation of the carrier and increased ionic strength, which can reduce the effective regeneration of active sites and decrease the overall transport flux. Similar trends have been reported by Ling and Suah (2017) and Ashraf *et al*. (2019), indicating that an optimum acid concentration is required to maintain efficient and continuous MG transport. FTIR characterization of the membrane before and after MG transport at varying HNO_3 concentrations in the receiving phase is shown in Figure 6.

Copyright © 2026, Universitas Sebelas Maret, ISSN 1412-4092, e ISSN 2443-4183

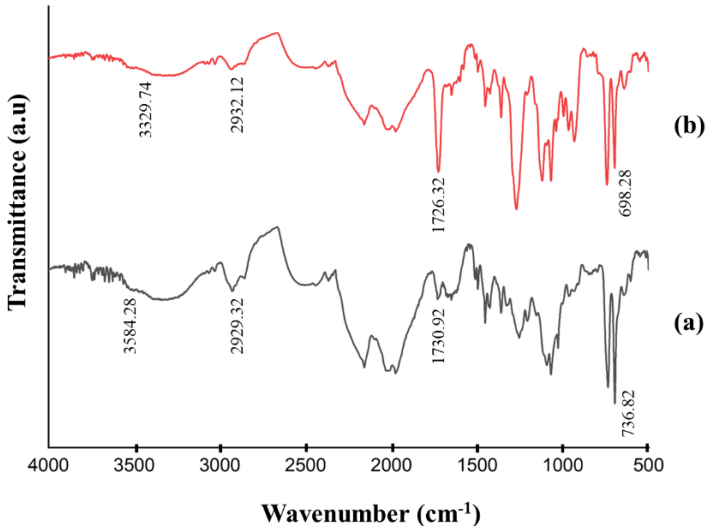


Figure 6. FTIR spectra of the membrane: (a) before transport, (b) after transport with varying HNO_3 concentrations in the receiving phase

Figure 6 shows a shift in the absorption band from 3584.28 cm^{-1} to 3329.74 cm^{-1}, indicating hydrogen bonding between the membrane and MG. The shift of the aliphatic C–H band from 2929.32 cm^{-1} to 2932.12 cm^{-1} and the C=O band from 1730.92 cm^{-1} to 1726.32 cm^{-1} indicates interactions between the polymer and MG (Kiswandono *et al*., 2024b). Additionally, the band at 736.62 cm^{-1} disappears and shifts to 689.28 cm^{-1}, showing aromatic structural involvement during transport. These changes confirm functional interactions between MG and the membrane without damaging the polymer structure.

Membrane Thickness Variation

PIM membranes were prepared in three thicknesses: thin (T_{27}), normal (T_{54}), and thick (T_{108}) (Table 3). Each membrane was installed in the transport pipe with 50 mL of 1.00 M HNO_3 as the receiving phase and 50 mL of 25 ppm MG solution at pH 7 as the source phase, stirred for 9 hours. The MG % removal was 67.50% (T_{27}), 80.02% (T_{54}), and 63.68% (T_{108}), with optimum efficiency at T_{54}. Thin membranes (T_{27}) had limited carrier content, reducing effectiveness, while thick membranes (T_{108}) increased diffusion resistance, lowering transport efficiency. These results are consistent with Kiswandono *et al*. (2024b), who stated that excessive thickness can hinder MG transport. The effect of membrane thickness on MG % removal is shown in Figure 7.

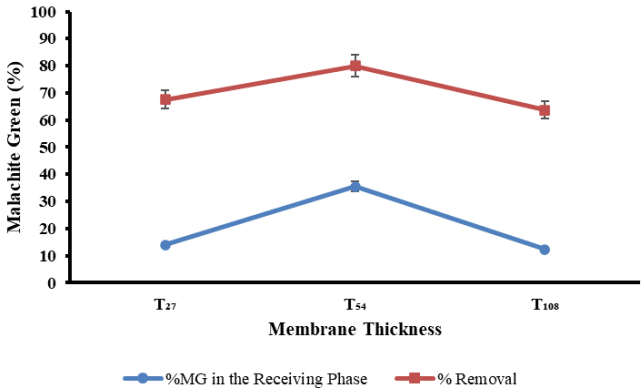


Figure 7. The effect of membrane thickness on the transported MG concentration.

Plasticizers play a crucial role in forming membrane structure and compactness. Low plasticizer content reduces viscosity, while excessive amounts increase membrane thickness and clog pores, thus hindering MG diffusion (Kiswandono *et al*., 2024b). In T_{108} membranes, excess plasticizer blocks interactions between MG and the carrier compound, reducing transport efficiency. Higher membrane viscosity results in lower MG transport rates (Kiswandono *et al*., 2024b). FTIR characterization of the membrane before and after MG transport at different membrane thicknesses is shown in Figure 8.

Copyright © 2026, Universitas Sebelas Maret, ISSN 1412-4092, e ISSN 2443-4183

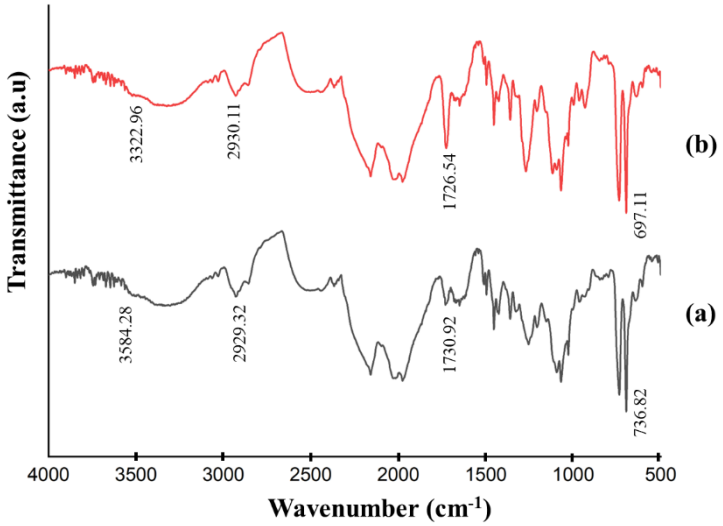


Figure 8. FTIR spectra of the membrane: (a) before transport (b) after transport with varying membrane thickness.

Based on the FTIR spectrum in Figure 8, the free –OH band at 3584.28 cm^{-1} before transport shifted to 3322.96 cm^{-1} after transport, indicating the formation of hydrogen bonds between the membrane and MG. The aliphatic C–H band shifted from 2929.32 cm^{-1} to 2930.11 cm^{-1}, and the C=O band shifted from 1730.92 cm^{-1} to 1726.54 cm^{-1}, showing dipole interactions and hydrogen bonding (Khairati *et al*., 2025). In the aromatic ring region, the band at 736.82 cm^{-1} shifted to 697.11 cm^{-1}, indicating aromatic interactions between MG and the membrane carrier. The optimum T54 membrane thickness allows maximum interaction and effective MG transport.

Carrier Compound Concentration Variation

PIM membranes with T_{54} thickness and various carrier amount (mmol) (Table 2) were installed in the transport pipe. The chamber was filled with 50 mL of 1.00 M HNO_3 as the receiving phase and 50 mL of 25 ppm MG solution as the source phase. The system was sealed and stirred with a magnetic stirrer for 9 hours. Carrier amount (mmol) variation aimed to examine its effect on MG transport optimization, as shown in Figure 9.

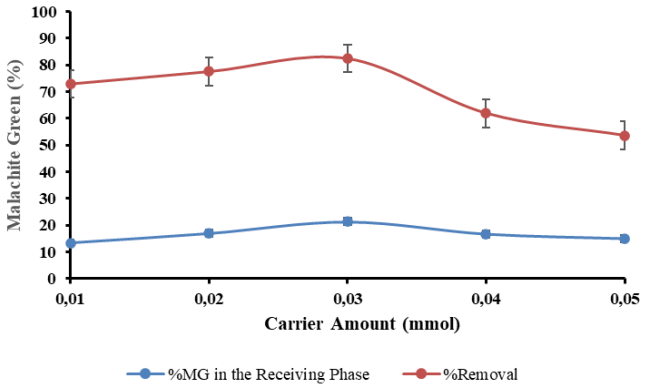


Figure 9. The Effect of carrier amount (mmol) on the transported MG concentration.

Transport results with carrier concentrations of 0.01, 0.02, 0.03, 0.04, and 0.05 mmol showed MG removal percentages of 72.95%, 77.57%, 82.45%, 61.99%, and 53.67%, respectively. The optimum concentration was 0.03 mmol, achieving the highest removal efficiency of 82.45%. The increase from 0.01 to 0.03 mmol was due to the additional –OH active groups in Co-EDVB 10%, which facilitated π–π interactions between MG and the aromatic structure in DVB (Kiswandono *et al*., 2022). However, further increases in carrier concentration (>0.03 mmol) resulted in decreased transport efficiency due to changes in membrane properties, such as increased membrane density and viscosity, which reduce membrane porosity and hinder MG diffusion and effective access to active sites (Kiswandono *et al*., 2024b). FTIR characterization of the membrane before and after MG transport at different carrier concentrations is shown in Figure 10.

Copyright © 2026, Universitas Sebelas Maret, ISSN 1412-4092, e ISSN 2443-4183

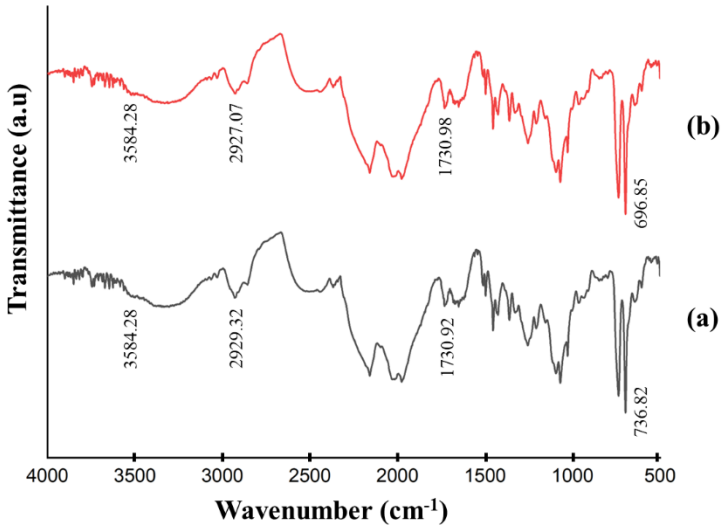


Figure 10. FTIR spectrum of the membrane (a) before transport and (b) after transport with variations in carrier compound concentration.

The FTIR spectra before (a) and after transport (b) showed shifts in absorption bands at 1730.92 cm^{-1} (C=O), 2929.32 cm^{-1} (–CH), and 3584.28 cm^{-1} (–OH), along with the appearance of a new band at 696.85 cm^{-1}. These changes indicate interactions between Co-EDVB and MG ions. The 0.03 mmol (0.0540 g) concentration proved optimal for MG transport without compromising membrane stability (Khairati *et al*., 2025).

Transport Time Variation

Transport time significantly affects MG transport efficiency. Longer interaction times increase the formation of hydrogen and π–π bonds between MG and the carrier compound (Kiswandono *et al*., 2022). The experiment was conducted under optimum conditions: source phase pH 7, HNO_3 concentration 1.00 M, T_{54} membrane, and 0.03 mmol carrier concentration. Transport times of 4, 8, 12, 18, and 24 hours resulted in MG removal percentages of 77.28%, 82.47%, 85.67%, 74.08%, and 71.69%, respectively. The optimum transport time was 12 hours. The effect of transport time on MG removal is presented in Figure 11.

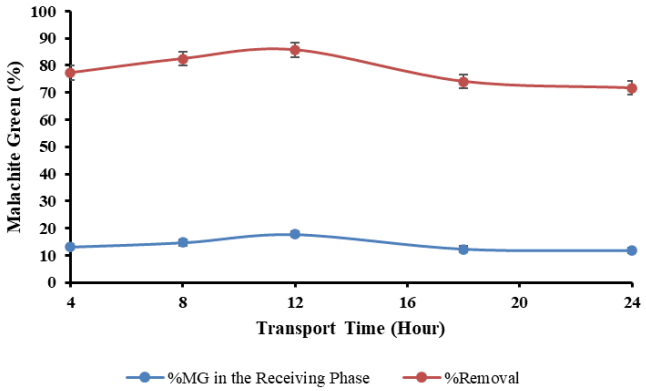


Figure 11. The effect of transport time on the transported concentration of MG.

Transport efficiency increased with time and reached a maximum at 12 hours, indicating effective interaction between MG and the carrier under optimum conditions. At longer transport times (18 – 24 hours), a moderate decrease in removal efficiency was observed. This behavior suggests the onset of gradual membrane instability, such as partial leaching of membrane components, which may reduce the availability of active sites and slightly limit transport flux. Importantly, this trend reflects a cumulative effect of prolonged operation rather than sudden membrane damage (Radzyminska-Lenarcik *et al*., 2020). SEM analysis was therefore conducted at the optimum transport time (12 hours) to represent membrane morphology under maximum performance conditions rather than to assess time-dependent degradation. FTIR characterization of the membrane before and after transport at different times is shown in Figure 12.

Copyright © 2026, Universitas Sebelas Maret, ISSN 1412-4092, e ISSN 2443-4183

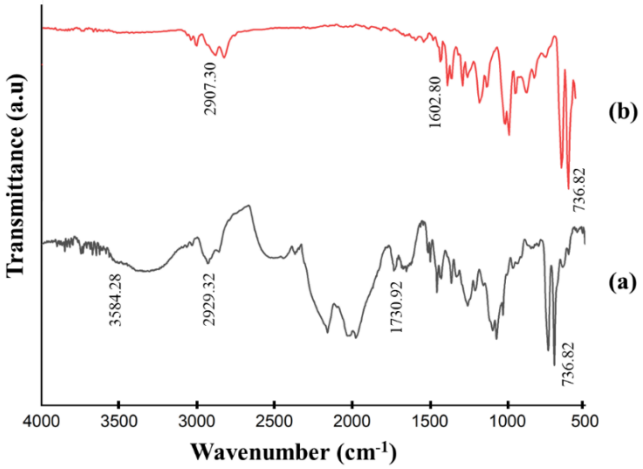


Figure 12. FTIR spectrum of the membrane (a) before transport (b) after transport with variations in transport time.

The FTIR spectrum before transport showed strong absorption bands at 3584.28 cm^{-1} (–OH group), 2929.32 cm^{-1} (aliphatic C–H), 1730.92 cm^{-1} (C=O), and 736.82 cm^{-1} (aromatic ring of eugenol). After 12 hours of transport, the –OH band at 3584.28 cm^{-1} disappeared, indicating interaction with MG. The C–H band shifted from 2929.32 cm^{-1} to 2907.30 cm^{-1}, and the C=O band shifted from 1730.92 cm^{-1} to 1602.80 cm^{-1}. The aromatic band at 736.82 cm^{-1} remained, confirming the stability of the aromatic structure (Khairati *et al*., 2025). Thus, 12 hours was the optimum transport time for effective MG transport.

Membrane characterization using SEM was conducted to observe surface morphology and pore distribution of the PIM membrane before and after transport. SEM analysis aimed to evaluate surface structure and potential changes during MG transport. The surface morphology of the PIM membrane containing Co-EDVB 10% before and after transport at the optimum time (12 hours) is shown in Figure 13.

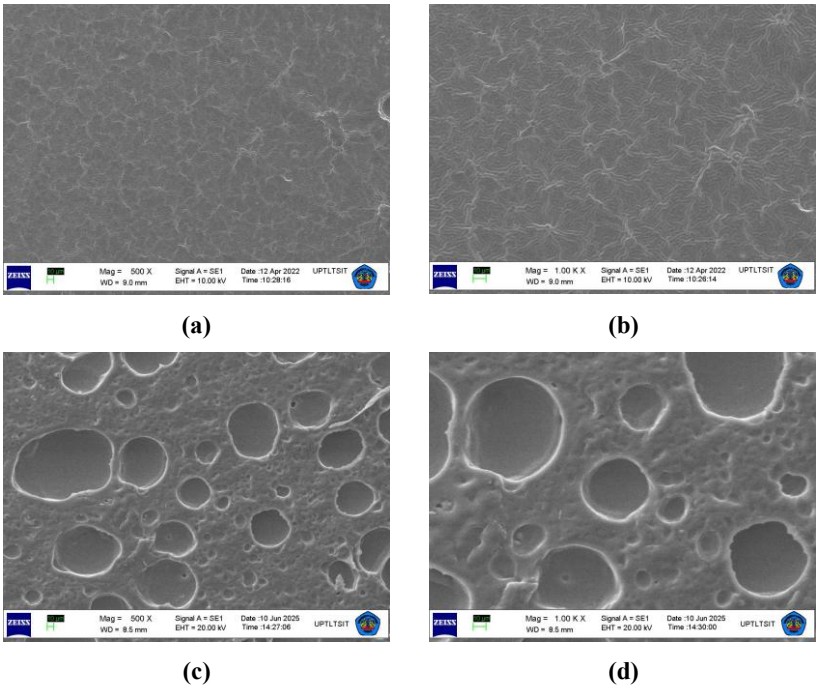


Figure 13. Surface morphology of the PIM membrane: (a) before transport at 500× magnification, (b) before transport at 1000× magnification, (c) after transport at 500× magnification, and (d) after transport at 1000× magnification at the optimum transport time (12 hours).

The PIM membrane surface before transport (a) showed a relatively homogeneous morphology with fine pores and a dense, intact surface. In contrast, the membrane after MG transport (b) exhibited a heterogeneous morphology with an uneven, fibrous surface. This change indicates that MG molecules dominated and expanded

Copyright © 2026, Universitas Sebelas Maret, ISSN 1412-4092, e ISSN 2443-4183

the membrane pores. This condition was likely influenced by leaching, the release of membrane components such as the carrier, base polymer, or plasticizer during transport. Leaching not only caused structural inhomogeneity but also altered pore distribution. According to Aprilia *et al*. (2025), this change allows MG molecules to occupy pores previously filled by leached components.

The PIM membrane containing 10% Co-EDVB exhibited a smooth and relatively dense surface before transport, while after the transport process, distinct and enlarged pores were clearly observed. These structures appear as well-defined cavities with clear boundaries, which are characteristic of pores rather than deposits or attached particles. If the observed features were magnesium carbonate adhering to the membrane surface, irregular agglomerates or surface coatings would be expected instead of open holes penetrating the membrane matrix. This observation is consistent with the morphological behavior of PIM membranes reported in previous studies. Compared to PIM membranes containing polyeugenol reported by Kiswandono *et al*. (2024a), which already exhibited large and homogeneous pores before use, the Co-EDVB-based membrane showed superior structural stability prior to transport. Polyeugenol, lacking a crosslinking agent, contains polar hydroxyl (–OH) groups that tend to phase-separate within the hydrophobic PVC matrix, leading to early pore formation. During transport, these pores enlarge irregularly due to interactions between the carrier and the transported solution.

In contrast, Co-EDVB utilizes divinylbenzene (DVB) as a crosslinking agent, forming a strongly crosslinked and hydrophobic polymer network. This structure results in a smooth membrane surface before transport and controlled pore enlargement after transport, indicating pore formation induced by component leaching rather than particulate attachment (Prasetya *et al.*, 2019). Therefore, the observed SEM features after transport can be confidently interpreted as pores formed within the membrane matrix, not magnesium carbonate adhering to or diffusing through the membrane.

CONCLUSION

Based on the results of the study, it can be concluded that the optimization of the PIM membrane for the transport of Malachite Green (MG) was achieved under the following conditions: a source phase pH of 7, 1 M HNO_3 as the receiving phase, the use of T_{54} membrane type, and the addition of 10% Co-EDVB carrier at a concentration of 0.03 mmol, with a transport duration of 12 hours. These conditions yielded optimal MG transport efficiency. The SEM characterization revealed an uneven, porous membrane surface, resulting from leaching during the transport process. This finding is supported by the FTIR results, which showed band shifts and decreased intensities, indicating chemical interactions between the membrane components and MG throughout the transport process.

CONFLICT OF INTEREST

The authors declare no conflict of interest. The funding sponsors had no role in the selection of the research topic; the design of the study; the collection, analysis, or interpretation of data; the writing of the manuscript; or the decision to publish the results.

AUTHOR CONTRIBUTION

AAK: Conceptualization, Methodology, Validation, Writing – Review and Editing, Visualization, Supervision, Project Administration, and Funding Acquisition; KCA: Conceptualization, Software, Formal Analysis, Investigation, Data Curation, Writing Original Draft Preparation, Visualization; RR: Validation, Software, and Resources; HIQ: Validation; SS: Writing – Review and Editing, Supervision.

ACKNOWLEDGEMENT

The author extends heartfelt appreciation to the Professorship Research Activity by the Budget Implementation List of the Public Service Agency (DIPA BLU) of the University of Lampung for their financial support. This support was provided under contract number 699/UN26.21/PN/2025.

DECLARATION OF GENERATIVE AI

During the preparation of this manuscript, the authors used Grammarly to assist with grammar checking and language editing. After using this tool, the authors reviewed and edited the content as necessary and take full responsibility for the content of the published article.

Copyright © 2026, Universitas Sebelas Maret, ISSN 1412-4092, e ISSN 2443-4183

REFERENCES

Abu-Hussien, S.H., Hemdan, B.A., Alzahrani, O.M., Alswat, A.S., Alatawi, F.A., Alenezi, M.A., Darwish, D.B.E., Bafhaid, H.S., Mahmoud, S.F., Ibrahim, M.F.M., and El-Sayed, S.M., 2022. Microbial Degradation, Spectral Analysis and Toxicological Assessment of Malachite Green Dye by *Streptomyces exfoliatus*. *Molecules*, 27. https://doi.org/10.3390/molecules27196456.

Aprilia, K.C., Safitri, N.U., Rakhman, K.A., and Kiswandono, A.A., 2025. Malachite Green Transport using Polymer Inclusion Membrane Method with Co-Edvb as Carrier. *Walisongo Journal of Chemistry*, 8, 87–97. https://doi.org/10.21580/wjc.v8i1.25826.

Arabi, H.R., Milani, S.A., Abolghasemi, H., and Zahakifar, F., 2021. Recovery and Transport of Thorium(IV) through Polymer Inclusion Membrane with D2EHPA from Nitric Acid Solutions. *Journal of Radioanalytical and Nuclear Chemistry*, 327, 653–665. https://doi.org/10.1007/s10967-020-07555-1.

Ashraf, W.M., Abulibdeh, N., and Salam, A., 2019. Selective Removal of Malachite Green Dye from Aqueous Solutions by Supported Liquid Membrane Technology. *International Journal of Environmental Research and Public Health*, 16. https://doi.org/10.3390/ijerph16183484.

Bahrami, S., Yaftian, M.R., Najvak, P., Dolatyari, L., Shayani-Jam, H., and Kolev, S.D., 2020. PVDF-HFP Based Polymer Inclusion Membranes Containing Cyphos® IL 101 and Aliquat® 336 for the Removal of Cr(VI) from Sulfate Solutions. *Separation and Purification Technology*, 250, 117251. https://doi.org/10.1016/j.seppur.2020.117251.

Benosmane, N., Boutemeur, B., Hamdi, S.M., and Hamdi, M., 2018. Removal of Phenol from Aqueous Solution Using Polymer Inclusion Membrane Based on Mixture of CTA and CA. *Applied Water Science*, 8. https://doi.org/10.1007/s13201-018-0643-8.

Carner, C.A., Croft, C.F., Kolev, S.D., and Almeida, M.I.G.S., 2020. Green Solvents for the Fabrication of Polymer Inclusion Membranes (PIMs). *Separation and Purification Technology*, 239, 116126. https://doi.org/10.1016/j.seppur.2019.116486.

Khairati, R.M., Kiswandono, A.A., Rinawati, R., and Ma'ruf, D.I., 2025. Application of Polymer Inclusion Membrane in the Transport of Malachite Green Dye Using Copolymer(Eugenol-Diallyl Phthalate) 2% as a Carrier. *Jurnal Kimia Sains dan Aplikasi*, 28, 8–15. https://doi.org/10.14710/jksa.28.1.8-15.

Kiswandono, A.A., Aprilia, K.C., Rahmawati, A., Widiarto, S., and Rinawati, 2024a. Evaluation of Polymer Inclusion Membrane Containing Copoly Eugenol Divinyl Benzene 10% as a Carrier for Phenol Transport. *Journal of Advanced Research in Fluid Mechanics and Thermal Sciences*, 122, 38–51. https://doi.org/10.37934/arfmts.122.2.3851.

Kiswandono, A.A., Mudasir, Siswanta, D., Aprilita, N.H., Santosa, S.J., and Hadi, S., 2020. Synthesis of a New Crosslinked Poly-Bisphenol a Diglycidyl Ether (Poly-BADGE) as a Carrier in Phenol Transport. *Kuwait Journal of Science*, 47, 39–48.

Kiswandono, A.A., Nusantari, C.S., Rinawati, R., and Hadi, S., 2022. Optimization and Evaluation of Polymer Inclusion Membranes Based on PVC Containing Copoly-EDVB 4% as a Carrier for the Removal of Phenol Solutions. *Membranes*, 12, 295. https://doi.org/10.3390/membranes12030295.

Kiswandono, A.A., Sindiani, A.V., Khotimah, R.K., Rabbani, M.B., Kurniawan, B., Rinawati, R., and Putra, H.E., 2024b. Transport of Malachite Green Using the Polyeugenol-Based Polymer Inclusion Membrane (PIM) Method. *Journal of Membrane Science and Research*, 10. https://doi.org/10.22079/JMSR.2023.2013382.1635.

Kowalewska, A., and Majewska-Smolarek, K., 2023. Eugenol-Based Polymeric Materials—Antibacterial Activity and Applications. *Antibiotics*. https://doi.org/10.3390/antibiotics12111570.

Ling, Y.Y., and Suah, F.B.M., 2017. Extraction of Malachite Green from Wastewater by Using Polymer Inclusion Membrane. *Journal of Environmental Chemical Engineering*, 5, 785–794. https://doi.org/10.1016/j.jece.2017.01.001.

Mazumder, N.A., and Rano, R., 2022. Preparation of Fly Ash-Ag2O Nanoaggregates as Highly Capable Photocatalyst for Malachite Green Dye Degradation under Solar Irradiation, in: *Materials Today: Proceedings*, 65, 2889–2893. https://doi.org/10.1016/j.matpr.2022.06.435.

Mohammed, M.A., Al-Bayati, I.S., Alobaidy, A.A., Waisi, B.I., and Majeed, N., 2023. Investigation the Efficiency of Emulsion Liquid Membrane Process for Malachite Green Dye Separation from Water. *Desalination and Water Treatment*, 307, 190–195. https://doi.org/10.5004/dwt.2023.29903.

Pathy, A., Krishnamoorthy, N., Chang, S.X., and Paramasivan, B., 2022. Malachite Green Removal Using Algal Biochar and Its Composites with Kombucha SCOBY: An Integrated Biosorption and Phycoremediation Approach. *Surfaces and Interfaces*, 30, 217–220. https://doi.org/10.1016/j.surfin.2022.101880.

Copyright © 2026, Universitas Sebelas Maret, ISSN 1412-4092, e ISSN 2443-4183

Prasetya, N.B.A., Ngadiwiyana, Ismiyarto, and Sarjono, P.R., 2019. Synthesis of Copolymer Eugenol Crosslinked with Divinyl Benzene and Preliminary Study on Its Antibacterial Activity, in: IOP Conference Series: Materials Science and Engineering, 509, 012102. https://doi.org/10.1088/1757-899X/509/1/012102.

Qiu, X. jing, Tang, J., Tan, J., Hu, H. ping, Ji, X. bo, and Hu, J. gang, 2021. Selective Recovery of Cu(II) through Polymer Inclusion Membranes Mediated with 2-Aminomethylpyridine Derivatives. *Transactions of Nonferrous Metals Society of China (English Edition)*, 31, 3591–3601. https://doi.org/10.1016/S1003-6326(21)65750-3.

Radzyminska-Lenarcik, E., Ulewicz, M., and Pyszka, I., 2020. Application of Polymer Inclusion Membranes Doped with Alkylimidazole to Separation of Silver and Zinc Ions from Model Solutions and after Battery Leaching. *Materials*, 13, 3103. https://doi.org/10.3390/ma13143103.

Raval, A.R., Kohli, H.P., and Mahadwad, O.K., 2022. Application of Emulsion Liquid Membrane for Removal of Malachite Green Dye from Aqueous Solution: Extraction and Stability Studies. *Chemical Engineering Journal Advances*, 12. https://doi.org/10.1016/j.ceja.2022.100398.

Sadiq, A.C., Olasupo, A., Rahim, N.Y., Ngah, W.S.W., Hanafiah, M.A.K.M., and Suah, F.B.M., 2023. Fabrication and Characterisation of Novel Chitosan-Based Polymer Inclusion Membranes and Their Application in Environmental Remediation. *International Journal of Biological Macromolecules*, 244. https://doi.org/10.1016/j.ijbiomac.2023.125400.

Soo, J.A.L., Shoparwe, N.F., Otitoju, T.A., Mohamad, M., Tan, L.S., Li, S., and Makhtar, M.M.Z., 2021. Characterization and Kinetic Studies of Poly(Vinylidene Fluoride-Co-Hexafluoropropylene) Polymer Inclusion Membrane for the Malachite Green Extraction. *Membranes*, 11. https://doi.org/10.3390/membranes11090676.

Copyright © 2026, Universitas Sebelas Maret, ISSN 1412-4092, e ISSN 2443-4183